Hyper-entanglement in a relativistic two-body system

2008 J. Phys. A: Math. Theor. 41 485302

(http://iopscience.iop.org/1751-8121/41/48/485302)

IOP PUBLISHING JOURNAL OF PHYSICS A: MATHEMATICAL AND THEORETICAL

J. Phys. A: Math. Theor. **41** (2008) 485302 (21pp) doi:10.1088/1751-8113/41/48/485302

Hyper-entanglement in a relativistic two-body system

A Bermudez and M A Martin-Delgado

Departamento de Física Teórica I, Universidad Complutense, 28040. Madrid, Spain

Received 15 July 2008, in final form 8 September 2008
Published 22 October 2008
Online at stacks.iop.org/JPhysA/41/485302

Abstract

We characterize the relativistic hyper-entanglement of two interacting massive fermions governed by the Dirac equation. In particular, we show how a certain Lorentz invariant coupling leads to the simultaneous entanglement of the fermionic spin and orbital degrees of freedom. Besides, this notion of hyper-entanglement turns out to be independent of the inertial reference frame. We also describe how this relativistic pairing mechanism leads to a bound fermionic pair which shows an interesting resemblance to a superconducting Cooper pair.

PACS numbers: 03.67.−a, 42.50.−p, 03.67.Mn, 03.65.Pm

(Some figures in this article are in colour only in the electronic version)

1. Introduction

The existence of correlations of a pure quantum mechanical nature can be considered as one of the most non-classical manifestations of quantum mechanics [1]. These singular quantum correlations, known as entanglement, have become an essential resource in the emerging fields of quantum information and computation [2, 3]. Entanglement is the key ingredient of various communication protocols, such as quantum teleportation, quantum dense coding, or secure quantum key distribution, and is believed to be necessary for the exponential speed-up of quantum algorithms. In this respect, it is extremely important to be able to detect, quantify and manipulate the entanglement of a certain system [4].

Remarkably, the characterization of entanglement in relativistic systems has revealed interesting properties which are absent in the usual non-relativistic regime [5]. In the absence of relativistic effects, it is possible to independently study the quantum correlations of discrete [6] or continuous [7] variable systems. This idealization is no longer possible in the relativistic domain since spin and orbital degrees of freedom become unavoidably mixed [8], and must be thus considered simultaneously. As a direct consequence, one is urged to reconsider and understand the peculiarities of entanglement in a relativistic framework. Recently, the entanglement of relativistic non-interacting particles, and its behavior under Lorentz transformations, has been extensively studied [9–14]. In the case of interacting particles, entanglement can be generated in scattering processes at lowest order QED [15, 16]. To the

best of our knowledge, there has not been a treatment of the generation of entanglement in interacting fermions described by the laws of relativistic quantum mechanics [17], and it is the main objective of this work to fill in such gap.

In this paper, we introduce a Lorentz invariant version of the Dirac equation for many-body systems [18], which allows a covariant treatment of interacting fermions. We shall focus on a paradigmatic two-fermion coupling which was historically introduced as an effective model of quark confinement [19–21]. Interestingly enough, we have found an insightful analytical solution which allows us to fully characterize the confining and entangling properties of this system. In particular, we have found that the system exhibits simultaneous entanglement in every degree of freedom, i.e. hyper-entanglement [22], which additionally is not affected by Lorentz transformations.

This paper is organized as follows. In section 2, we introduce a covariant formulation of the Dirac equation for many-fermion systems and describe the main features of the interacting two-body system that shall be studied throughout this work. In section 3, we derive a complete analytical solution of the system, describing in detail the energy spectrum and associated eigenstates. We also analyze the consequences of indistinguishability, which surprisingly lead to non-classical effects, such as squeezing or anti-bunching [23]. In section 4, we describe hyper-entanglement in the spin and orbital degrees of freedom of these two relativistic fermions. We show that any finite coupling leads to simultaneous spin and orbital entanglement, and the system is thus hyper-entangled. Besides, we argue that these quantum correlations are invariant under Lorentz transforms, and therefore the hyper-entanglement has an invariant meaning. Finally, we review in appendix A the notion of $SU(2)$ coherent states [24] which arise in the description of the relativistic eigenstates. Additionally, in appendix B, we describe the confining properties of this system and describe an interesting analogy with Cooper pairs in superconducting materials [25].

2. Relativistic two-body Hamiltonian

The properties of a free relativistic spin-1/2 fermion of mass m can be described by means of the Dirac equation

$$(\gamma^\mu p_\mu - mc)|\Psi\rangle = 0, \tag{1}$$

where $|\Psi\rangle$ stands for a Dirac spinor, $p_\mu = \mathrm{i}\hbar(c^{-1}\partial_t, \boldsymbol{\nabla})$ is the 4-momentum operator, $\hbar$ stands for the Planck constant, and c for the speed of light. Here, γ^μ are the well-known Dirac matrices which fulfil a Clifford algebra

$$\{\gamma^\mu, \gamma^\nu\} = 2g^{\mu\nu}, \tag{2}$$

where $g^{\mu\nu} = \mathrm{diag}(1, -1, -1, -1)$ is the Minkowski metric tensor. Such algebra (2) may be satisfied with the following choice of Dirac matrices, known as the standard representation, $\gamma^0 := \beta = \mathrm{diag}(\mathbb{I}_2, -\mathbb{I}_2)$, and $\gamma^j := \gamma^0\alpha_j$ with $\alpha_j = \text{off-diag}(\sigma_\mathrm{j}, \sigma_\mathrm{j})$ and σ_j as the usual Pauli matrices [17].

Let us mention here that the following non-minimal coupling $\mathbf{p} \to \mathbf{p} - \mathrm{i}m\omega\beta\mathbf{r}$ leads to a relativistic extension of the usual harmonic oscillator, the so-called Dirac oscillator, where ω represents its frequency [19, 20]. Nonetheless, the extension of such coupling to many-fermion systems is not straightforward since one must preserve the Lorentz invariance of the generalized Dirac equation. In this regard, the following Lorentz scalars [18] must be introduced

$$\Gamma = \prod_{n=1}^{N} \left(\gamma_n^\mu u_\mu\right), \qquad \Gamma_n = \left(\gamma_n^\mu u_\mu\right)^{-1}\Gamma, \tag{3}$$

where $u_\mu = (-P_\mu P_\mu)^{-1/2} P_\mu$ is a time-like vector defined in terms of the total 4-momentum $P_\mu = \sum_{n=1}^{N} p_{\mu n}$, N represents the total number of fermions, and the many-body Dirac matrices become $\gamma_n^\mu = \mathbb{I} \otimes \mathbb{I} \cdots \mathbb{I} \otimes \gamma^\mu \otimes \mathbb{I} \cdots \mathbb{I}$. The non-minimal coupling $\mathbf{p} \to \mathbf{p} - \mathrm{i}m\omega\beta\mathbf{r}$ can now be extended in a Lorentz invariant fashion, yielding the following relativistic equation:

$$\sum_{n=1}^{N} \left[\Gamma_n\left(\gamma_n^\mu (p_{\mu n} - \mathrm{i}m\omega_n \tilde{x}_{\mu n}\Gamma) + mc\right)\right]|\Psi\rangle = 0, \tag{4}$$

where we introduce different frequencies for each fermion ω_n. As a requirement of Lorentz invariance, the position operators $x_{\mu n}$ should be modified under the following prescription $x_{\mu n} \to \tilde{x}_{\mu n} = (x_{\mu n} - X_\mu) - u_\mu (P^\nu (x_{\nu n} - X_\nu))$, with $X_\mu = N^{-1} \sum_{n=1}^{N} x_{\mu n}$ as the center of mass coordinates. This Dirac equation describes the properties of systems of many relativistic fermions, and has attracted a considerable amount of attention since it effectively describes quark confinement. In the particular case of light mesons (i.e. $N = 2$ and $\omega_1 = -\omega_2$), this equation accounts for the confinement of a quark–antiquark pair [21]. Unfortunately, it cannot be completely solved and one must resign with perturbative [26] or partial non-perturbative solutions [27]. However, these solutions exhibit many of the properties of real mesons, such as excitation energies [26, 27].

In this paper we shall be concerned with the confinement of two identical fermions (i.e. $N = 2$ and $\omega_1 = \omega_2 := \omega$), where we have derived a complete analytical solution that allows an insightful discussion of the confining and entanglement properties of this system. In the center of mass reference frame[1], the relativistic equation (4) leads to the following Hamiltonian:

$$H = \frac{c}{\sqrt{2}}(\boldsymbol{\alpha}_1 - \boldsymbol{\alpha}_2)(\mathbf{p} - \mathrm{i}m\omega\beta_{12}\mathbf{r}) + mc^2(\beta_1 + \beta_2), \tag{5}$$

where $\boldsymbol{\alpha}_1 = \boldsymbol{\alpha} \otimes \mathbb{I}_4$, $\boldsymbol{\alpha}_2 = \mathbb{I} \otimes \boldsymbol{\alpha}$, $\beta_1 = \beta \otimes \mathbb{I}$, $\beta_2 = \mathbb{I} \otimes \beta$, and $\beta_{12} = \beta \otimes \beta$ represent the generalization of the Dirac matrices in the two-body Hilbert space. Here $\mathbf{p} := (\mathbf{p}_1 - \mathbf{p}_2)/\sqrt{2}$, and $\mathbf{r} := (\mathbf{r}_1 - \mathbf{r}_2)/\sqrt{2}$ stand for relative momentum and position operators. If we restrict to a (2+1)-dimensional Minkowski spacetime, the Dirac matrices reduce to the usual Pauli matrices $\alpha_x = \sigma_x$, $\alpha_y = \sigma_y$, $\beta = \sigma_z$, and the Hamiltonian can be written as follows:

$$H = \frac{c}{\sqrt{2}} \sum_{j=x,y} (\sigma_j \otimes \mathbb{I}_2 - \mathbb{I}_2 \otimes \sigma_j)(p_j - \mathrm{i}m\omega\sigma_z \otimes \sigma_z r_j) + mc^2(\sigma_z \otimes \mathbb{I}_2 + \mathbb{I}_2 \otimes \sigma_z). \tag{6}$$

In the forthcoming sections, we shall describe in detail the properties of this interesting compound fermionic system. Indeed, this system provides an ideal scenario where to study the effective confinement, and relativistic bipartite entanglement.

3. Complete analytical solution

3.1. Beyond quantum optical models

Recently, several single-fermion relativistic models [28–31] have been related to archetypical models in quantum optics [23]. In this context, it is possible to find exact mappings between the relativistic Hamiltonians and the Jaynes–Cummings (JC) coupling [32], a fundamental Hamiltonian that describes the interaction between a two-level atom and a quantized mode

[1] The advantage of a Lorentz invariant formulation of this many-body Dirac equation is that we can study its solution in any given inertial frame and afterwards relate them by means of simple Lorentz transformations. In particular, the center of mass frame $u_\mu = (1, 0, 0, 0)$ is the optimal choice to obtain the analytical solution and also to study the hyper-entanglement of the eigenstates [8].

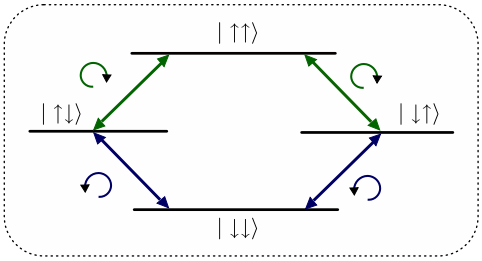

Figure 1. Relativistic coupling scheme: fermionic spin-flip transitions mediated by the creation or annihilation of chiral quanta. Due to the relativistic coupling described in equation (8), there are two possible spin-flip channels of opposed chirality. Namely, $|\uparrow\downarrow\rangle|n_l\rangle \leftrightarrow |\uparrow\uparrow\rangle|n_l+1\rangle \leftrightarrow |\downarrow\uparrow\rangle|n_l\rangle$ is a left-handed channel , whilst $|\uparrow\downarrow\rangle|n_r\rangle \leftrightarrow |\downarrow\downarrow\rangle|n_r+1\rangle \leftrightarrow |\downarrow\uparrow\rangle|n_r\rangle$ is a right-handed one. According to equations (9) and (10), both channels conserve the total angular momentum.

of the electromagnetic (EM) field. Besides, one also finds mappings onto the anti-Jaynes–Cummings (AJC) interaction [33], an essential ingredient that appears in the field of trapped ions [34]. This astonishing connection between relativistic quantum mechanics and quantum optics has turned out to be extremely fruitful, since several relativistic phenomena have been predicted using the tools of quantum optics. In this section, we argue that these mappings cannot be obtained for the two-body Hamiltonian introduced in equation (5). In order to describe the relativistic Hamiltonian, one must go beyond the standard quantum optical models.

In two-dimensions, the chiral creation-annihilation operators[2], which carry dual aspects of the left- and right-handed symmetry, can be defined as follows:

$$\begin{aligned} a_r &:= \tfrac{1}{\sqrt{2}}(a_x - \mathrm{i}a_y), \qquad & a_r^\dagger &:= \tfrac{1}{\sqrt{2}}\big(a_x^\dagger + \mathrm{i}a_y^\dagger\big), \\ a_l &:= \tfrac{1}{\sqrt{2}}(a_x + \mathrm{i}a_y), \qquad & a_l^\dagger &:= \tfrac{1}{\sqrt{2}}\big(a_x^\dagger - \mathrm{i}a_y^\dagger\big), \end{aligned} \tag{7}$$

where $a_x^\dagger, a_x, a_y^\dagger, a_y$, are the cartesian creation-annihilation operators of the harmonic oscillator $a_j^\dagger = \frac{1}{\sqrt{2}}\big(\frac{1}{\tilde{\Delta}} r_j - \mathrm{i}\frac{\tilde{\Delta}}{\hbar} p_j\big)$, and $\tilde{\Delta} = \sqrt{\hbar/m\omega}$ sets the length scale of the system. Using these operators, the relativistic Hamiltonian (6) takes a simpler and amenable form

$$H = \begin{bmatrix} \Delta & g^* a_l^\dagger & g a_l^\dagger & 0 \\ g a_l & 0 & 0 & g^* a_r \\ g^* a_l & 0 & 0 & g a_r \\ 0 & g a_r^\dagger & g^* a_r^\dagger & -\Delta \end{bmatrix}, \tag{8}$$

where $\Delta := 2mc^2$ is related to the system rest mass energy, and $g := \mathrm{i}mc^2\sqrt{2\xi}$ controls the strength of the effective interaction, with $\xi := \hbar\omega/mc^2$. Considering the two-body spinorial basis $\{|\uparrow\uparrow\rangle, |\uparrow\downarrow\rangle, |\downarrow\uparrow\rangle, |\downarrow\downarrow\rangle\}$, we can understand the relativistic two-body coupling as a four-level system depicted in figure 1. There, we can see how the transitions between the different spinorial components are always mediated through the creation or annihilation of chiral quanta. The particular combination of the chiral operators is demanded by the conservation of the total angular momentum

$$J_z = S_z + L_z, \tag{9}$$

where we have introduced the z-component of the total spin and angular momentum operators

$$L_z := \hbar\big(a_r^\dagger a_r - a_l^\dagger a_l\big), \qquad S_z := \sigma_z \otimes \mathbb{I}_2 + \mathbb{I}_2 \otimes \sigma_z. \tag{10}$$

[2] Note that these chiral operators describe collective modes of the system, since they are defined in terms of the relative position and momentum operators $\mathbf{p} := (\mathbf{p}_1 - \mathbf{p}_2)/\sqrt{2}$ and $\mathbf{r} := (\mathbf{r}_1 - \mathbf{r}_2)/\sqrt{2}$.

Let us now compare the relativistic Hamiltonian (8) with quantum optical models describing the interaction of two-level atoms with quantized modes of the EM field. Since the relativistic Hamiltonian contains a couple of spin-1/2 particles coupled to a pair of chiral modes, we should compare it to a quantum optical model involving a pair of two-level atoms coupled to two modes of EM radiation. The most general quantum optical interaction[3] can be described as

$$H = \Delta(\sigma_{z1} + \sigma_{z2}) + \sum_{jk} \left(g_{jk}^{\mathrm{JC}} \sigma_j^+ b_k + g_{jk}^{\mathrm{AJC}} \sigma_j^+ b_k^\dagger + \mathrm{h.c.} \right), \tag{11}$$

where $b_1^\dagger, b_1, b_2^\dagger, b_2$ stand for the creation-annihilation operators of the EM field modes, g_{jk}^{JC} $\left(g_{jk}^{\mathrm{AJC}}\right)$ is the coupling constant corresponding to a Jaynes–Cummings (anti-Jaynes–Cummings) interaction between the jth atom and the kth mode [32–34], and Δ is the detuning. This Hamiltonian (11) can be understood as a generalization of the usual Tavis–Cummings model which describes atoms interacting with a single mode of the EM field [35]. In order to find an exact mapping between Hamiltonians in equations (8), and (11), the coupling constants g_{jk} must fulfil the following constraints:

$$\begin{aligned} &g_{11}^{\mathrm{JC}} + \mathrm{i} g_{12}^{\mathrm{JC}} = 0, \qquad && g_{11}^{\mathrm{JC}} - \mathrm{i} g_{12}^{\mathrm{JC}} = 0, \\ &g_{21}^{\mathrm{JC}} + \mathrm{i} g_{22}^{\mathrm{JC}} = 0, && g_{21}^{\mathrm{JC}} - \mathrm{i} g_{22}^{\mathrm{JC}} = 0, \\ &g_{11}^{\mathrm{AJC}} + \mathrm{i} g_{12}^{\mathrm{AJC}} = 0, && g_{11}^{\mathrm{AJC}} - \mathrm{i} g_{12}^{\mathrm{AJC}} = 0, \\ &g_{21}^{\mathrm{AJC}} + \mathrm{i} g_{22}^{\mathrm{AJC}} = 0, && g_{21}^{\mathrm{AJC}} - \mathrm{i} g_{22}^{\mathrm{AJC}} = 0, \end{aligned} \tag{12}$$

which only present the trivial solution $g_{jk}^{\mathrm{JC}} = g_{jk}^{\mathrm{AJC}} = 0$. Therefore, we may conclude that the relativistic Hamiltonian cannot be mapped onto any generalized two-mode two-atom Tavis–Cummings model. In this respect, this singular two-body coupling goes beyond standard quantum optics.

3.2. Relativistic energy spectrum and eigenstates

In the previous section we have proved that the Hamiltonian in (8) cannot be expressed in terms of well-known quantum optical models. Nonetheless, as we shall discuss in this section, it is still possible to find the complete energy spectrum and corresponding eigenstates. Therefore, this two-fermion relativistic system belongs to the small class of exactly solvable few-body relativistic models. Let us introduce the chiral Fock states

$$|n_r, n_l\rangle := \frac{1}{\sqrt{n_r! n_l!}} \left(a_r^\dagger\right)^{n_r} \left(a_l^\dagger\right)^{n_l} |\mathrm{vac}\rangle, \tag{13}$$

where $n_r, n_l = 0, 1, \ldots$ specify the number of right- and left-handed quanta in the two-fermion system. It is essential to realize that the Hilbert space can be divided in a series of invariant subspaces $\mathcal{H} = \bigoplus_{n_r,n_l=0}^{\infty} \mathcal{H}_{n_r n_l}$, where each subspace $\mathcal{H}_{n_r n_l} := \mathcal{H}'_{n_r,n_l} \bigoplus \mathcal{H}''_{n_r,n_l}$ can be spanned as follows:

$$\begin{aligned} \mathcal{H}'_{n_r,n_l} &= \mathrm{span}\{|+\rangle|\mathrm{n_r}, \mathrm{n_l}\rangle\}, \\ \mathcal{H}''_{n_r,n_l} &= \mathrm{span}\{|\uparrow\uparrow\rangle|\mathrm{n_r}, \mathrm{n_l}+1\rangle, |-\rangle|\mathrm{n_r}, \mathrm{n_l}\rangle, |\downarrow\downarrow\rangle|\mathrm{n_r}+1, \mathrm{n_l}\rangle\}, \end{aligned} \tag{14}$$

Here we have introduced the maximally entangled depolarized Bell states $|-\rangle := (|\uparrow\downarrow\rangle - |\downarrow\uparrow\rangle)/\sqrt{2}$, and $|+\rangle := (|\uparrow\downarrow\rangle + |\downarrow\uparrow\rangle)/\sqrt{2}$ [37].

[3] The most general interaction between $N-$ atoms and $M-$ modes has been studied in [36]. In our case, we should restrict to two-modes and two-atoms. Besides, due to the indistinguishability of fermions, the atoms and the modes are restricted to present the same energy (i.e. $\Delta E = \hbar\omega_0$ sets the atomic energy scale, whereas ω sets the modes frequency).

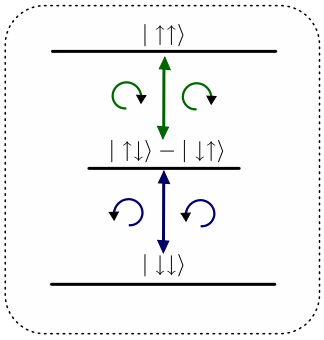

Figure 2. Effective three-level relativistic coupling scheme: in the invariant subspace $\mathcal{H}''_{n_r,n_l}$, the effective Hamiltonian in equation (15) induces spin-flip transitions between three different levels. Namely, a left-handed AJC interaction induces $|\uparrow\uparrow\rangle|n_r, n_l+1\rangle \leftrightarrow |-\rangle|n_r, n_l\rangle$, whilst a right-handed JC interaction is responsible for $|-\rangle|n_r, n_l\rangle \leftrightarrow |\downarrow\downarrow\rangle|n_r+1, n_l\rangle$.

Remarkably, $\mathcal{H}'_{n_r,n_l}$ describes a zero-energy subspace $E_{+n_r n_l} = 0$, whose states $|+\rangle|n_r, n_l\rangle$ can neither absorb nor emit phonons, they are effectively trapped. This trapping effect occurs due to the destructive quantum interference between the transitions taking place through different channels (see figure 1). Therefore, these states are the relativistic analogue of the so-called dark states in the quantum optical domain, which lie at the heart of significant effects such as coherent trapping [38], or electromagnetically induced transparency [39]. The Hamiltonian (8) in the remaining subspaces $\mathcal{H}''_{n_r,n_l}$ can be expressed as follows:

$$H_{\text{eff}} = \Delta \begin{bmatrix} 1 & -\mathrm{i}\sqrt{\xi(n_l+1)} & 0 \\ \mathrm{i}\sqrt{\xi(n_l+1)} & 0 & -\mathrm{i}\sqrt{\xi(n_r+1)} \\ 0 & \mathrm{i}\sqrt{\xi(n_r+1)} & -1 \end{bmatrix}. \tag{15}$$

Here, the two-body interaction couples three different levels in a ladder configuration by means of left-handed AJC interaction $|\uparrow\uparrow\rangle|n_r, n_l+1\rangle \leftrightarrow |-\rangle|n_r, n_l\rangle$, and a right-handed JC interaction $|-\rangle|n_r, n_l\rangle \leftrightarrow |\downarrow\downarrow\rangle|n_r+1, n_l\rangle$ (see figure 2).

This insightful three-level perspective allows us to exactly diagonalize the two-body relativistic Hamiltonian (6). Using Cardano–Vietta solution to third-order polynomials, we obtain the following energies:

$$\begin{aligned} E_{+n_r n_l} &:= 0, \\ E_{j n_r n_l} &:= \Delta\sqrt{\frac{4\,[1+\xi(n_r+n_l+2)]}{3}}\cos\Theta_{j n_r n_l}, \end{aligned} \tag{16}$$

where the index $j = 1, 2, 3$ refers to the different energy levels, and

$$\Theta_{j n_r n_l} := \frac{1}{3}\cos^{-1}\left[\frac{27(n_l-n_r)\xi}{2\,[3(1+\xi(n_r+n_l+2))]^{3/2}}\right] + \frac{2\pi}{3}(j-1). \tag{17}$$

These eigenstates are represented for different values of the relative coupling strength parameter ξ in figures 3 and 4.

Once the eigenvalues have been obtained, we may derive the corresponding eigenstates, which we list below

$$\begin{aligned} |E_{+n_r n_l}\rangle &:= |+\rangle|n_r, n_l\rangle, \\ |E_{j n_r n_l}\rangle &:= \frac{1}{\Omega_{j n_r n_l}}(\mathrm{i}\beta_{j n_r n_l}|\uparrow\uparrow, n_r, n_l+1\rangle \\ &\quad + \alpha_{j n_r n_l}|-\rangle|n_r, n_l\rangle + \mathrm{i}\delta_{j n_r n_l}|\downarrow\downarrow, n_r+1, n_l\rangle), \end{aligned} \tag{18}$$

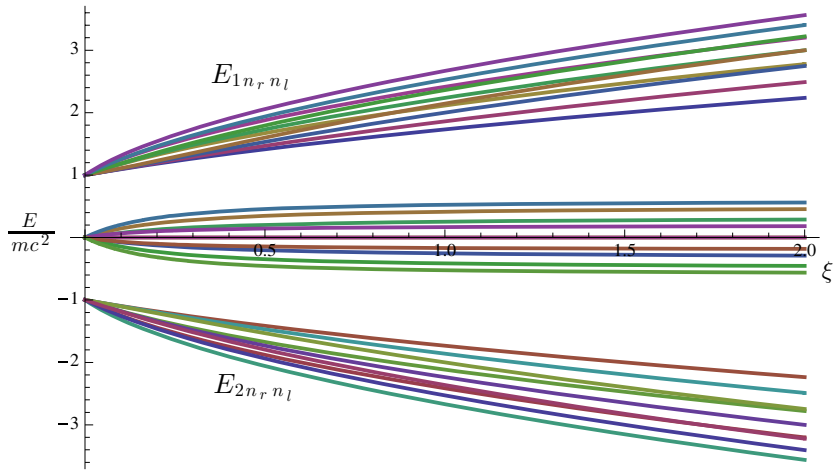

Figure 3. Energy spectrum of the relativistic system: representation of the relativistic energy levels for the first excited states described in equation (16) as a function of the coupling strength ξ. Here, we observe that the levels corresponding to $E_{1n_r n_l}$, and $E_{2n_r n_l}$ are clearly discernible, they correspond to the external upper and lower branches respectively. Conversely, levels $E_{3n_r n_l}$, and $E_{+n_r n_l}$ are clearer seen in figure 4

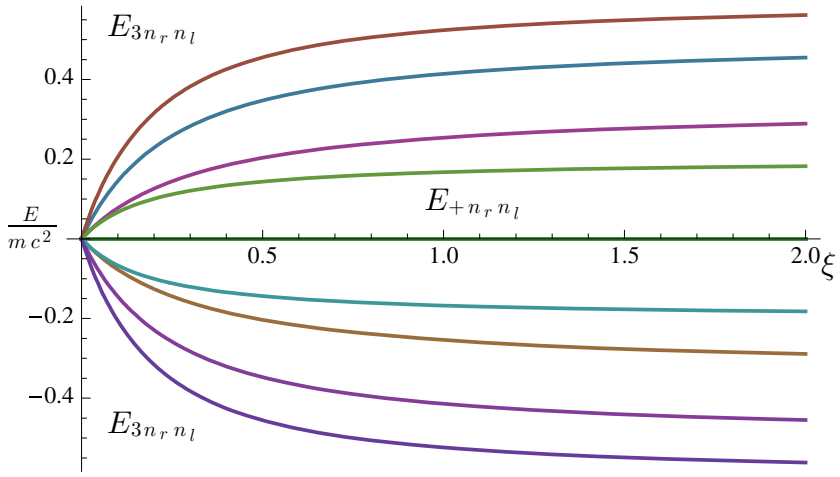

Figure 4. Detailed low-energy spectrum of the relativistic system: representation of the first excited states corresponding to levels $E_{3n_r n_l}$ and $E_{+n_r n_l}$. We clearly observe that the $E_{+n_r n_l} = 0$, while the remaining levels $E_{3n_r n_l}$ lie above or below the zero-energy branch.

where we have defined the following parameters:

$$\begin{aligned}
\alpha_{jn_r n_l} &:= \Delta^2 - E^2_{jn_r n_l}, \\
\beta_{jn_r n_l} &:= \Delta(\Delta + E_{jn_r n_l})\sqrt{\xi(n_l + 1)}, \\
\delta_{jn_r n_l} &:= \Delta(\Delta - E_{jn_r n_l})\sqrt{\xi(n_r + 1)}, \\
\Omega_{jn_r n_l} &:= \sqrt{\alpha^2_{jn_r n_l} + \beta^2_{jn_r n_l} + \delta^2_{jn_r n_l}}.
\end{aligned} \tag{19}$$

Here the indexes $j = 1, 2, 3$ correspond to the three different eigenvalues (16). We have thus derived a complete solution of the relativistic Dirac equation of two bodies interacting via a Dirac oscillator coupling. As stated previously, we have proved that this system belongs to the scarcely populated class of exactly solvable few-body systems in relativistic quantum mechanics.

3.3. Fermion indistinguishability

Once the exact energy spectrum (16) with its corresponding eigenstates (18) have been derived, we must consider the consequences of fermion indistinguishability. The symmetrization postulate states that a system of identical fermions must be described in terms of anti-symmetrical states. Therefore, the whole Hilbert space $\mathcal{H} = \bigoplus_{n_r,n_l=0}^{\infty} \mathcal{H}_{n_r n_l}$ contains states which are not physically acceptable. Physical states must satisfy the following condition

$$\mathrm{P}_{21}|\Psi(1,2)\rangle = -|\Psi(1,2)\rangle, \tag{20}$$

where P_{21} stands for the permutation operator that swaps the fermion labels $1 \leftrightarrow 2$. Considering the eigenstates in equation (18) under the permutation operator, we obtain the following expressions:

$$\begin{aligned} \mathrm{P}_{21}|E_{+,n_r,n_l}\rangle &= (-1)^{n_r+n_l}|E_{+,n_r,n_l}\rangle, \\ \mathrm{P}_{21}|E_{j\ ,n_r,n_l}\rangle &= (-1)^{n_r+n_l+1}|E_{+,n_r,n_l}\rangle. \end{aligned} \tag{21}$$

Since these expressions must satisfy the antisymmetric condition in equation (20), the number of chiral quanta are constrained as follows:

$$\begin{aligned} |E_{+,n_r,n_l}\rangle &\Rightarrow n_r + n_l = 2k+1 \qquad : k = 0, 1, 2, \ldots \\ |E_{j\ ,n_r,n_l}\rangle &\Rightarrow n_r + n_l = 2k \qquad\ : k = 0, 1, 2, \ldots. \end{aligned} \tag{22}$$

Due to the indistinguishability of the relativistic fermions, the eigenstates $|E_{+,n_r,n_l}\rangle$ must contain an odd number of chiral quanta, whereas $|E_{j,n_r,n_l}\rangle$ are restricted to even number of chiral quanta. Thus, fermion indistinguishability imposes essential constraints on the allowed two-particle states which may lead to measurable results. As will be shown in section 4, the two-body relativistic version of Glauber coherent states [40] can be identified with even and odd coherent states [41] which present measurable non-classical aspects such as squeezing or anti-bunching [23]. It is interesting to note that similar effects in a non-relativistic framework require additional non-linearities in the Hamiltonian, whereas in this relativistic regime they arise as a consequence of the fermion statistics.

Before concluding this section, we must also describe how the indistinguishable character of the fermions also affects the nature of physical observables. Identical fermions share the same physical properties, and therefore acceptable physical observables $\mathrm{O}(1, 2)$ cannot depend on the particle labels. Consequently, physical observables in a system of indistinguishable must be symmetric under the permutation operator

$$\mathrm{P}_{21}\mathrm{O}\,(1,2)\mathrm{P}_{21}^{\dagger} = \mathrm{O}(1,2) \Rightarrow [\mathrm{O}(1,2), \mathrm{P}_{21}] = 0. \tag{23}$$

From the two-body Dirac oscillator in equation (6), we immediately see that

$$\left[H_{\mathrm{DO}}^{\mathrm{2D}}, \mathrm{P}_{21}\right] = 0, \tag{24}$$

and thus we can guarantee its symmetric nature. Furthermore, this property also shows that the permutation operator and the relativistic Hamiltonian have common eigenstates (21). It is exactly this property which gives rise to the peculiar subdivision of the invariant subspaces $\mathcal{H}_{n_r n_l} := \mathcal{H}'_{n_r,n_l} \bigoplus \mathcal{H}''_{n_r,n_l}$ in equation (14), and the existence of the so-called relativistic dark states.

4. Relativistic hyper-entanglement

In this section, we report on the relativistic entanglement properties of the eigenstates described in equations (18). Remarkably enough, these states are simultaneously entangled in every degree of freedom (i.e. hyper-entangled). The concept of hyper-entanglement was introduced for photons [22] in order to outperform Bell state analysis [42] and has been experimentally tested [43]. In this section we generalize hyper-entanglement to massive particles, spin-1/2 relativistic fermions, where the system becomes simultaneously entangled in spin and orbital degrees of freedom. We further investigate the regimes where it is possible to obtain maximal hyper-entanglement.

Let us remark here the relativistic invariant meaning of the results to be described below. In a seminal paper by Peres *et al* [8], an intriguing relativistic effect was discussed, namely, the notion of spin entropy for a relativistic free fermion is not invariant under Lorentz transformations. This fact leads to a non-invariant notion of spin and momentum entanglement for pairs of free fermions [10], which would lead to a dubious concept of hyper-entanglement. However, as we shall justify below, the particular eigenstates of the two-fermion system considered in this paper belong to a decoherence-free-subspace under the action of Lorentz boosts [45]. Hence, we can define an invariant spin and orbital entanglement by means of the von Neumann entropy of the corresponding reduced density matrices.

4.1. Bipartite description of the eigenstates

Before embarking upon the characterization of hyper-entanglement, it is convenient to express the system eigenstates in the bipartite Hilbert space $\mathcal{H} = \mathcal{H}_1 \otimes \mathcal{H}_2$. Hence, the collective chiral operators in equation (7) must be expressed in terms of one-body operators

$$\begin{aligned} a_r &= \tfrac{1}{\sqrt{2}}(a_{1r} - a_{2r}), \qquad & a_r^\dagger &= \tfrac{1}{\sqrt{2}}\left(a_{1r}^\dagger - a_{2r}^\dagger\right), \\ a_l &= \tfrac{1}{\sqrt{2}}(a_{1l} - a_{2l}), \qquad & a_l^\dagger &= \tfrac{1}{\sqrt{2}}\left(a_{1l}^\dagger - a_{2l}^\dagger\right), \end{aligned} \tag{25}$$

where the indexes in $\left\{a_{j\alpha}, a_{j\alpha}^\dagger\right\}$ stand for the $j = 1, 2$ fermion, whereas $\alpha = r, l$ refers to the mode chirality. These one-body operators satisfy the usual bosonic algebra

$$[a_{j\alpha}, a_{k\beta}] = \left[a_{j\alpha}^\dagger, a_{k\beta}^\dagger\right] = 0, \qquad \left[a_{j\alpha}, a_{k\beta}^\dagger\right] = \delta_{\alpha\beta}\delta_{jk}, \tag{26}$$

which allow us to rewrite the collective chiral Fock state in equation (13) as follows:

$$|n_r, n_l\rangle = \sum_{m_r=0}^{n_r} \sum_{m_l=0}^{n_l} C_{m_r m_l}^{n_r n_l} |n_r - m_r, n_l - m_l\rangle_1 |m_r, m_l\rangle_2, \tag{27}$$

where we have introduced the following constants in terms of the usual binomial coefficients (see equation (A.5) in appendix A)

$$C_{m_r m_l}^{n_r n_l} = \frac{1}{\sqrt{2^{n_r+n_l}}} \binom{n_r}{m_r}^{\frac{1}{2}} \binom{n_l}{m_l}^{\frac{1}{2}} (-1)^{m_r+m_l}. \tag{28}$$

As discussed in appendix A, these states are a particular instance of $SU(2)$ coherent states [24], which are the $SU(2)$ Lie algebra generalization of the usual Glauber coherent states [40]. These coherent states posses many non-classical properties, such as sub-Poissonian statistics in the chiral phononic ensemble [44], but we will now focus on their bipartite entanglement.

4.2. Entanglement in the spin degree of freedom

As mentioned previously, entanglement is an essential resource in quantum information protocols which must be quantified. To accomplish such task, there are different measures that capture complementary aspects of entanglement [4]. Nevertheless, in the case of pure bipartite states, it suffices to obtain the entropy of entanglement since any other measure coincides with the latter in the asymptotic limit. The entropy of entanglement is defined as the von Neumann entropy of the reduced density matrix

$$\mathcal{E}(\rho) = -\mathrm{tr}_1(\rho_1 \log_2 \rho_1) = -\mathrm{tr}_2(\rho_2 \log_2 \rho_2), \tag{29}$$

where $\rho = |\psi_{12}\rangle\langle\psi_{12}|$ is the density matrix corresponding to the pure bipartite state $|\psi_{12}\rangle \in \mathcal{H}_1 \otimes \mathcal{H}_2$, and $\rho_1 = \mathrm{tr}_2(\rho)$, $\rho_2 = \mathrm{tr}_1(\rho)$ stand for the reduced density matrices.

In particular, if we want to characterize the entanglement in the spin degree of freedom, we should previously trace over the orbital degrees of freedom. The reduced spin density matrices , associated with the eigenstates in equation (18)

$$\begin{aligned}
\rho^{\mathrm{spin},1}_{+n_r n_l} &= \frac{1}{2}|\uparrow\rangle\langle\uparrow| + \frac{1}{2}|\downarrow\rangle\langle\downarrow|, \\
\rho^{\mathrm{spin},1}_{jn_r n_l} &= \frac{|\alpha_{jn_r n_l}|^2 + 2|\beta_{jn_r n_l}|^2}{2\Omega^2_{jn_r n_l}}|\uparrow\rangle\langle\uparrow| + \frac{|\alpha_{jn_r n_l}|^2 + 2|\gamma_{jn_r n_l}|^2}{2\Omega^2_{jn_r n_l}}|\downarrow\rangle\langle\downarrow|,
\end{aligned} \tag{30}$$

where the matrices $\rho^{\mathrm{spin},1}_{+n_r n_l} = \mathrm{tr}_2(\mathrm{tr}_{\mathrm{orb}}|E_{+n_r n_l}\rangle\langle E_{+n_r n_l}|)$, $\rho^{\mathrm{spin},1}_{jn_r n_l} = \mathrm{tr}_2(\mathrm{tr}_{\mathrm{orb}}|E_{jn_r n_l}\rangle\langle E_{jn_r n_l}|)$, and we are using the normalization parameters introduced in equation (19). The corresponding entropy of entanglement can be obtained using equation (29)

$$\begin{aligned}
\mathcal{E}^{\mathrm{spin}}_{+n_r n_l} &= 1 \\
\mathcal{E}^{\mathrm{spin}}_{jn_r n_l} &= -\log_2\left(1 - \lambda^{\mathrm{spin}}_{jn_r n_l}\right) - \lambda^{\mathrm{spin}}_{jn_r n_l}\log_2\left(\frac{\lambda^{\mathrm{spin}}_{jn_r n_l}}{1 - \lambda^{\mathrm{spin}}_{jn_r n_l}}\right),
\end{aligned} \tag{31}$$

where we have introduced the following parameter $\lambda^{\mathrm{spin}}_{jn_r n_l} := (|\alpha_{jn_r n_l}|^2 + 2|\beta_{jn_r n_l}|^2)/2\Omega^2_{jn_r n_l}$. It is important to point out that the maximum spin entanglement is bounded by $\mathcal{E}^{\mathrm{spin}}_{max} = \log_2(d_{\mathrm{spin}}) = 1$, where $d_{\mathrm{spin}} = 2$ is the dimension of the Hilbert space corresponding to the spin degrees of freedom (i.e. the density matrices correspond to effective qubits). Hence, it follows from equations (31) that the eigenstate $|E_{+n_r n_l}\rangle$ is maximally entangled independently of the coupling strength ξ. Conversely, in the strong coupling limit $1 \ll \xi \lesssim 2$, the eigenstates $\{|E_{jn_r n_l}\rangle\}$ are only partially entangled and show an interesting dependence of the coupling ξ as shown in figure 5. In the weak coupling regime $\xi \ll 1$, it is possible to extract two states $\{|E_{+n_r n_l}\rangle, |E_{3n_r n_l}\rangle\}$ which are already maximally entangled. Conversely, in the strong coupling regime, every state is entangled but only partially. In this respect, we may conclude that the degree of spin entanglement is highly sensitive to the coupling strength between the two bodies.

4.3. Entanglement in the orbital degrees of freedom

As mentioned in the introduction, one distinctive feature of relativistic systems is that both discrete and continuous variables are present in the description of entanglement. Whilst the spin degree of freedom is associated with discrete variables, continuous variables must be related to the orbital degrees of freedom. In this case, the Hilbert space dimension is infinite and the quantification of entanglement becomes rather intricate [7]. In the quantum information scenario, many of the continuous variable states belong to the relevant family of Gaussian states, where many tools on entanglement characterization have been developed.

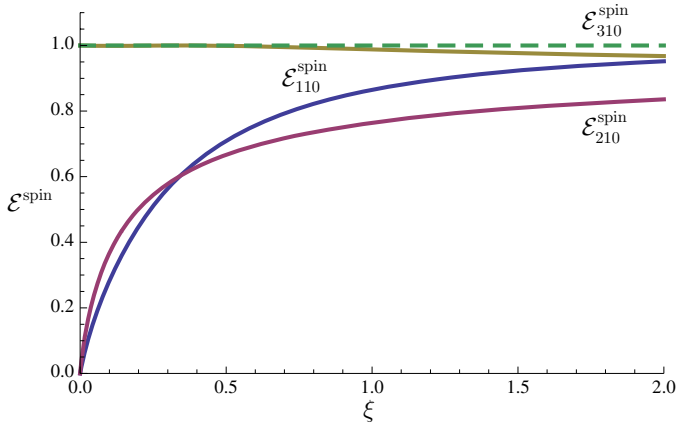

Figure 5. Spin entropy of entanglement: the spin entanglement of the eigenstates $\{|E_{jn_rn_l}\rangle\}$ with the lowest number of quanta (i.e. $n_r = 1, n_l = 0$) is represented as a function of the relativistic coupling strength ξ. In the weak coupling scenario $\xi \ll 1$, there is a drastic decrease of entanglement of states $\{|E_{1,n_rn_l}\rangle, |E_{2,n_rn_l}\rangle\}$, whereas the entanglement of $|E_{3,n_rn_l}\rangle$ attains the maximum possible value. In the strong coupling regime $1 \ll \xi \lesssim 2$, the eigenstates are not maximally entangled but show a high degree of quantum correlations. Note that the dashed line corresponds to the bound of maximal entanglement for a pair of qubits $\mathcal{E}^{\rm spin}_{max} = 1$.

Unfortunately, the relativistic states considered in this work are not Gaussian and therefore different techniques must be used.

In this section we characterize orbital entanglement by means of the entropy of entanglement introduced in equation (29), where we need to additionally trace over the spin degrees of freedom in the reduced density matrices $\rho^{\rm orb,1}_{+n_rn_l} = {\rm tr}_2({\rm tr}_{\rm spin}|E_{+n_rn_l}\rangle\langle E_{+n_rn_l}|)$, and $\rho^{\rm orb,1}_{jn_rn_l} = {\rm tr}_2({\rm tr}_{\rm spin}|E_{jn_rn_l}\rangle\langle E_{jn_rn_l}|)$

$$\rho^{\rm orb,1}_{+n_rn_l} = \sum_{m_r=0}^{n_r}\sum_{m_l=0}^{n_l} \lambda^{\rm orb}_{+m_rm_l} P^{+}_{m_r,m_l}, \qquad \rho^{\rm orb,1}_{jn_rn_l} = \sum_{m_r=0}^{n_r+1}\sum_{m_l=0}^{n_l+1} \lambda^{\rm orb}_{jm_rm_l} P^{j}_{m_r,m_l}. \tag{32}$$

Here, we have introduced the associated projectors

$$\begin{aligned} P^{+}_{m_r,m_l} &:= |n_r - m_l, n_l - m_l\rangle_1\langle n_r - m_r, n_l - m_l|_1, \\ P^{j}_{m_r,m_l} &:= |n_r + 1 - m_l, n_l + 1 - m_l\rangle_1\langle n_r + 1 - m_r, n_l + 1 - m_l|_1, \end{aligned} \tag{33}$$

and the following important parameters:

$$\begin{aligned} \lambda^{\rm orb}_{+m_rm_l} &= \left|C^{n_rn_l}_{m_rm_l}\right|^2, \\ \lambda^{\rm orb}_{j00} &= 0, \\ \lambda^{\rm orb}_{j01} &= \frac{\left|\delta_{jn_rn_l}\right|^2}{2^{n_r+n_l+1}\Omega^2_{jn_rn_l}}, \\ \lambda^{\rm orb}_{j10} &= \frac{\left|\beta_{n_rn_l}j\right|^2}{2^{n_r+n_l+1}\Omega^2_{jn_rn_l}}, \\ \lambda^{\rm orb}_{jm_rm_l} &= \frac{1}{\Omega^2_{jn_rn_l}}\left(\left|\alpha_{jn_rn_l}\right|^2\left|C^{n_rn_l}_{m_r-1m_l-1}\right|^2 + |\beta_{jn_rn_l}|^2\left|C^{n_rn_l+1}_{m_r-1m_l}\right|^2 + \left|\delta_{jn_rn_l}\right|^2\left|C^{n_r+1n_l}_{m_rm_l-1}\right|^2\right), \end{aligned} \tag{34}$$

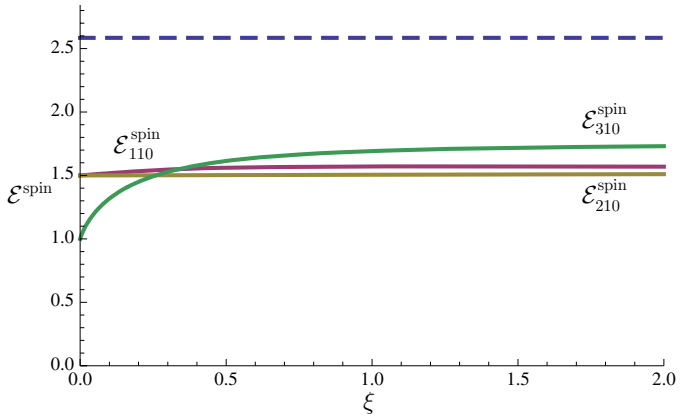

Figure 6. Orbital entropy of entanglement: the orbital entanglement of the eigenstates $\{|E_{jn_rn_l}\rangle\}$ with the lowest number of quanta (i.e. $n_r = 1, n_l = 0$) is represented as a function of the relativistic coupling strength ξ. The states $\{|E_{1,n_rn_l}\rangle, |E_{2,n_rn_l}\rangle\}$ are nearly insensitive to the coupling strength, whereas the entanglement of $|E_{3,n_rn_l}\rangle$ increases as we enter the strong coupling regime $1 \ll \xi \lesssim 2$. Note that the dashed line corresponds to the bound of maximal entanglement for this pair of qudits $\mathcal{E}^{\text{spin}}_{max} = \log_2 3$, which shows that the orbital degree of freedom is not maximally entangled.

where we have used the previously introduced parameters of equations (19) and (28). It is important to note that although the orbital degrees of freedom correspond to continuous variables, the reduced density matrices in equation (32) have finite dimension. In this respect, they correspond to an effective qudit of dimension $d^{\text{orb}}_{+n_rn_l} = (n_r + 1)(n_l + 1)$, and $d^{\text{orb}}_{jn_rn_l} = (n_r + 2)(n_l + 2)$, whose entropy quantifies entanglement as follows:

$$\begin{aligned}\mathcal{E}^{\text{orb}}_{+n_rn_l} &= -\sum_{m_r=0}^{n_r}\sum_{m_l=0}^{n_l} \lambda^{\text{orb}}_{+m_rm_l}\log_2\lambda^{\text{orb}}_{+m_rm_l},\\ \mathcal{E}^{\text{orb}}_{jn_rn_l} &= -\sum_{m_r=0}^{n_r+1}\sum_{m_l=0}^{n_l+1} \lambda^{\text{orb}}_{jm_rm_l}\log_2\lambda^{\text{orb}}_{jm_rm_l}.\end{aligned} \tag{35}$$

The orbital entropy of entanglement is fully characterized by equations (34)–(35), which show that the orbital entanglement of $|E_{+n_rn_l}\rangle$ is also independent of the coupling strength ξ. The orbital entropy of entanglement of states $\{|E_{jn_rn_l}\rangle\}$ has been depicted in figure 6 as a function of the two-body coupling strength. With respect to the spin entropy of entanglement (figure 5), we observe two main differences. Namely, the orbital degree of freedom is not so sensitive to the coupling strength, and the states are only partially entangled.

4.4. Hyper-entanglement in a relativistic system

As introduced previously, hyper-entanglement between two particles occurs whenever they are simultaneously entangled in various degrees of freedom. With the results from previous sections at hand, we can make the main statement of this work, namely, hyper-entanglement in spin and orbital degrees of freedom can be generalized to relativistic massive fermions. It follows from figures 5 and 6 that any eigenstate of the system is simultaneous entangled in spin and orbital degrees of freedom for $\xi > 0$,

$$0 < \mathcal{E}^{\text{spin}}_{\alpha,n_r,n_l} \leqslant 1, \qquad 0 < \mathcal{E}^{\text{orb}}_{\alpha,n_r,n_l} \leqslant \log_2 d^{\text{orb}}_{\alpha n_rn_l}, \tag{36}$$

where we have introduced $\alpha \in \{+, 1, 2, 3\}$.

The results presented so far have been obtained in the center of mass inertial frame, also known as the Lorentz rest frame. This particular inertial frame was proposed as a special frame where an invariant definition of entanglement could be derived [8]. It was later shown that the spin and orbital degree of entanglement is not Lorentz invariant, namely, Lorentz transformations transfer entanglement between the spin and orbital degrees of freedom [10]. In this respect, the concept of relativistic hyper-entanglement must be revisited and its Lorentz invariance deserves a more detailed study.

Let us say a few words about the invariance meaning of the two-body relativistic hyper-entanglement introduced in this work. From the results in [10], one would expect the degree of spin and orbital entanglement in equations (31) and (35), and thus the notion of hyper-entanglement, to be modified under Lorentz boost. Nonetheless, it has been proved that the states $\{|n_r, n_l\rangle_1, |n_r, n_l\rangle_2\}$ belong to invariant subspaces with respect to Lorentz transformations [45]. Since these states are the building blocks of our relativistic eigenstates (see equation (27)), we might conclude that this relativistic system provides us with a physical implementation of Lorentz-decoherence-free subspaces (i.e. there is no decoherence or loss of entanglement due to Lorentz boosts) [46, 47]. As a direct result, we expect no transfer of entanglement between the spin and orbital degrees of freedom to occur in this relativistic two-body system, and therefore we can claim that the notion of relativistic hyper-entanglement presented here does not depend on the inertial reference frame.

5. Conclusions

In this work, we have studied the confinement and entanglement properties in a relativistic two-fermion system described by the Dirac equation. We have thoroughly described how to generalize the Dirac equation to many-body systems maintaining its Lorentz covariance. In the particular case of an interacting system where the fermions are non-minimally coupled through a relativistic spring, we have obtained a complete analytical solution. In this respect, the two-dimensional two-fermion Dirac oscillator belongs to the small class of exactly solvable few-fermion systems. Additionally, we have seen how a series of quantum optical concepts such as dark states, and coherent trapping, or important non-classical effects such as squeezing, anti-bunching and sub-Poissonian statistics arise in this relativistic setting.

The analytical expressions for the two-fermion eigenstates allowed us to fully characterize the entanglement properties of this system. We have studied the rise of quantum correlations in the spin and orbital degrees of freedom as a consequence of the relativistic coupling. Furthermore, these correlations are simultaneous for any finite interaction, and therefore we may claim that the fermions are hyper-entangled. We have also argued that this relativistic extension of the concept of hyper-entanglement to massive relativistic fermions has a Lorentz invariant meaning, and therefore is independent of the inertial frame to be considered. To the best of our knowledge, these are the first results on the entanglement of interacting fermions governed by the Dirac equation.

Some other additional properties have been left to the appendices, where we have shown that the bipartite eigenstates are expressed in terms of generalized $SU(2)$ coherent states, which allow us to interpret the full relativistic coupling as a double Mach–Zehnder interferometer. In the appendices, we have as well discussed the effective confinement that the non-minimal coupling provides. Surprisingly, we have brought out several analogies with superconducting Cooper pairs. Although the pairing mechanism arises from different mechanism, this relativistic compound system shows an interesting resemblance to the pairing of electrons in superconducting materials.

Appendix A. $SU(2)$ coherent states

In this appendix we review the properties of two-mode $SU(2)$ coherent states, which can also be found in the literature as spin coherent states. These states were introduced as a generalization of the usual Glaubler coherent states [40] for arbitrary Lie groups [24, 48, 49]. In this case, we shall restrict our attention to the $SU(2)$ group, whose generators $\{J_+, J_-, J_3\}$ have the following Lie algebra:

$$[J_3, J_\pm] = \pm J_\pm, \qquad [J_+, J_-] = 2J_3. \tag{A.1}$$

The generators of this algebra (A.1) can be expressed in terms of the single-particle chiral bosonic operators described in equations (25), where we find the following chiral Schwinger representations:

$$\begin{aligned} J_3^r &= \tfrac{1}{2}\big(a_{1r}^\dagger a_{1r} - a_{2r}^\dagger a_{2r}\big), \qquad & J_+^r &= a_{1r}^\dagger a_{2r} = (J_-^r)^\dagger \\ J_3^l &= \tfrac{1}{2}\big(a_{1l}^\dagger a_{1l} - a_{2l}^\dagger a_{2l}\big), \qquad & J_+^l &= a_{1l}^\dagger a_{2l} = (J_-^l)^\dagger. \end{aligned} \tag{A.2}$$

The Lie algebraic commutators in equation (A.1) follow directly from the bosonic commutation relations in equations (26). The $SU(2)$ coherent states are defined by means of the generalized displacement operator of the corresponding $SU(2)$ Lie algebra, which might be disentangled using the results in [48]

$$\begin{aligned} U_{z,r} &= \mathrm{e}^{z(J_+^r - J_-^r)} = \mathrm{e}^{-\tan|z| J_+^r}\, \mathrm{e}^{\log(\cos^{-2}|z|) J_3^r}\, \mathrm{e}^{\tan|z| J_-^r}, \\ U_{z,l} &= \mathrm{e}^{z(J_+^l - J_-^l)} = \mathrm{e}^{-\tan|z| J_+^l}\, \mathrm{e}^{\log(\cos^{-2}|z|) J_3^l}\, \mathrm{e}^{\tan|z| J_-^l}, \end{aligned} \tag{A.3}$$

where we restrict to $z \in \mathbb{R}$. Once the displacement operator has been factorized, we can easily obtain the right- and left-handed $SU(2)$ coherent states as the displaced vacuum[4]

$$\begin{aligned} |z, n_r\rangle &= \cos^{n_r}|z| \sum_{m_r=0}^{n_r} \binom{n_r}{m_r} (-\tan|z|)^{m_r} |n_r - m_r\rangle_1 |m_r\rangle_2, \\ |z, n_l\rangle &= \cos^{n_l}|z| \sum_{m_l=0}^{n_l} \binom{n_l}{m_l} (-\tan|z|)^{m_l} |n_l - m_l\rangle_1 |m_l\rangle_2, \end{aligned} \tag{A.4}$$

with the usual binomial coefficients

$$\binom{n}{m} = \frac{n!}{(n-m)!m!}. \tag{A.5}$$

$SU(2)$ coherent states become experimentally accessible in the field of quantum optics [50, 51], where parametric processes allow the required transformation of photons between different modes in equation (A.4). In the relativistic setting, they arise naturally as the eigenstates of the two-body Hamiltonian (6) for specific choice of the parameter $z = \pi/4$,

$$\begin{aligned} |\pi/4, n_r\rangle &= \frac{1}{\sqrt{2^{n_r}}} \sum_{m_r=0}^{n_r} \binom{n_r}{m_r} (-1)^{m_r} |n_r - m_r\rangle_1 |m_r\rangle_2, \\ |\pi/4, n_l\rangle &= \frac{1}{\sqrt{2^{n_l}}} \sum_{m_l=0}^{n_l} \binom{n_l}{m_l} (-1)^{m_l} |n_l - m_l\rangle_1 |m_l\rangle_2, \end{aligned} \tag{A.6}$$

[4] The Lie algebraic vacuum is defined as $J_-^r|\mathrm{vac}\rangle = 0$, and therefore corresponds to $|\mathrm{vac}\rangle = |\mathrm{n_r}\rangle_1 |0\rangle_2$ (idem for J_-^l). In this regard, the corresponding vacuum can be interpreted as a chiral Fock state in the first particle mode, whereas the usual bosonic vacuum in the second particle mode.

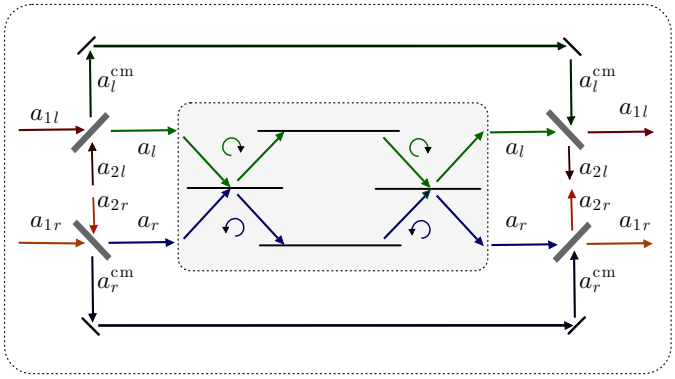

Figure A1. Double Mach–Zehnder interferometer: the initial beam splitters convert the incoming single-particle modes $\{a_{j\alpha}, a_{j\alpha}^{\dagger}\}$ into collective modes corresponding to the relative and center of mass coordinates. The center of mass modes evolve without dephasing inside the interferometer (i.e. free particle Hamiltonian), whereas the modes corresponding to the relative coordinates are subjected to a dephasing caused by their coupling to the spinorial levels (i.e. interacting Hamiltonian). The final beam splitters recombine the modes to express the solution in the bipartite Hilbert space.

which coincide with the chiral Fock states in relative coordinates that appear in equation (27)

$$|n_r, n_l\rangle = \sum_{m_r=0}^{n_r} \sum_{m_l=0}^{n_l} C_{m_r m_l}^{n_r n_l} |n_r - m_r, n_l - m_l\rangle_1 |m_r, m_l\rangle_2, \tag{A.7}$$

where we have introduced the following constants:

$$C_{m_r m_l}^{n_r n_l} := \frac{1}{\sqrt{2^{n_r+n_l}}} \binom{n_r}{m_r} \binom{n_l}{m_l} (-1)^{m_r+m_l}. \tag{A.8}$$

It is also interesting to point out that the generalized displacement operator in equation (A.3), particularized to $z = \pi/4$, can be interpreted as a simple $50:50$ quantum beam splitter [52] that is mixing the chiral bosonic modes

$$U_{\frac{\pi}{4},r} = \mathrm{e}^{\frac{\pi}{4}(a_{1r}^{\dagger} a_{2r} - a_{1r} a_{2r}^{\dagger})} \qquad U_{\frac{\pi}{4},l} = \mathrm{e}^{\frac{\pi}{4}(a_{1l}^{\dagger} a_{2l} - a_{1l} a_{2l}^{\dagger})}. \tag{A.9}$$

Hence, $SU(2)$ coherent states can be simply obtained applying a $50:50$ beam splitter to a single Fock state populating one mode. This observation allows us to reinterpret the relativistic Hamiltonian in equation (5) in terms of a double Mach–Zehnder interferometer (see figure A1).

Appendix B. Lorentz invariant confinement

As discussed previously, the non-minimal coupling introduced in equation (4) effectively describes quark confinement in hadrons. In the particular case of mesons (i.e. $N = 2$, and $\omega_1 = -\omega_2$), this equation accounts for the confinement of a quark–antiquark pair [21] and predicts many of the properties of real mesons, such as excitation energies [26, 27]. In this section, we shall be concerned with the confinement of two identical fermions subjected to the Hamiltonian in equation (6). Surprisingly, we find many analogies between this Lorentz invariant pairing mechanism and the pairing of electrons in superconducting materials [25, 53, 54]. However, let us clarify that the origin of these pairings is completely different.

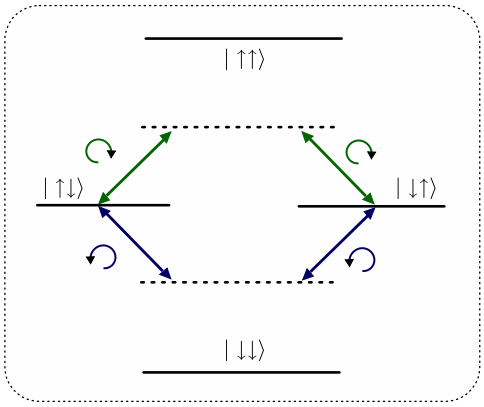

Figure B1. Fermionic spin-flip transitions in the weak coupling regime: the low energy sector is described by an effective two-level system, where spin-flips occur along two different channels that include virtual two-phonon transitions and spin-polarized states become decoupled.

On the one hand, pairing in superconductors arises as a many-body effect where the lattice phonons and the Fermi sea provide the essential ingredients. On the other hand, the relativistic pairing is introduced as an effective coupling in equation (4), and therefore we deal with a single two-body system.

Below, we describe the resemblance of these relativistic fermionic pairs and the usual Cooper pairs in BCS theory [25, 54]. We have found that, in analogy to the pairing of Cooper pairs, binding occurs regardless of the interaction strength. Additionally, we have found a similar scaling of the energy gap in the weak coupling regime, which allows us to identify the relativistic ω with the lattice phonon Debye frequency ω_D in superconductors. Besides, the relativistic bound pairs are also in a spin singlet state, and present a spherically symmetric onion-like structure in the probability distribution. On the other hand, a strong interaction leads to remarkable differences with respect to BCS Cooper pairs. In this case, more than one bound pair can be built, which in any case is not in a singlet state but rather in a linear superposition of singlet and triplet states. Furthermore, phonons become unfrozen as the coupling strength is raised and dynamically contribute to the pairing mechanism.

B.1. Weak coupling regime

The standard description of Cooper pairs in superconducting solids is usually performed in a weak coupling regime, where a slightly phonon-mediated attractive interaction binds electrons which lay close to the Fermi surface. We shall thus consider the relativistic two-fermion Hamiltonian in equation (6) in such limit of weak coupling $\xi \ll 1$. In this regime, the spin-polarized levels become decoupled from those responsible for the low-energy properties (see figure B1).

The effective Hamiltonian describing the weak coupling in the low-energy sector can be obtained by adiabatic elimination of the spin polarized levels $\{|\uparrow\uparrow\rangle, |\downarrow\downarrow\rangle\}$ as follows:

$$H_{\text{eff}} := \hbar\omega\left(a_r^\dagger a_r - a_l^\dagger a_l\right)\begin{bmatrix} 1 & -1 \\ -1 & 1 \end{bmatrix}, \tag{B.1}$$

where the allowed transitions can take on two different channels via the consecutive creation-annihilation of right- or left-handed phonons. This process can be understood as an instance

of a superexchange coupling between the spins $|\uparrow\downarrow\rangle \longleftrightarrow |\downarrow\uparrow\rangle$ driven by a second-order two-phonon process where a chiral phonon is virtually created and then annihilated. There exist two different exchange paths, as seen in figure B1, depending on the left- or right-handed chiralities of the virtual phonons involved in the process. This effective Hamiltonian (B.1) can be exactly diagonalized yielding the eigenvalues

$$E^{\text{eff}}_{+n_r n_l} := 0, \qquad E^{\text{eff}}_{-n_r n_l} := 2\hbar\omega\,(n_r - n_l), \tag{B.2}$$

with the following associated eigenstates

$$\begin{aligned} |E^{\text{eff}}_{+n_r n_l}\rangle &:= |+, n_r, n_l\rangle \Rightarrow n_r + n_l = 2k+1 \qquad : k = 0, 1, 2, \ldots \\ |E^{\text{eff}}_{-n_r n_l}\rangle &:= |-, n_r, n_l\rangle \Rightarrow n_r + n_l = 2k \qquad\quad : k = 0, 1, 2, \ldots, \end{aligned} \tag{B.3}$$

where the anti-symmetric character of the fermionic states has already been considered. Therefore, the low-lying solution in the weak coupling regime can be described by the maximally entangled Bell states in the spin degree of freedom, and chiral Fock states in the orbital degree of freedom.

Furthermore, these states describe a bound fermion pair. In order to show that such binding occurs, we must show that the inter-particle distance only attains finite values. Let us introduce the square-distance operator $\Gamma := x^2 + y^2$, where $x := (x_1 - x_2)/\sqrt{2}$ and $y := (y_1 - y_2)/\sqrt{2}$ denote the space coordinate operators for the relative fermionic distance. Note that this operator is physically acceptable since is satisfies the constraint in equation (23). The expectation values in the weak-coupling eigenstates (B.3) are

$$\langle\Gamma\rangle_{\pm} = \frac{\tilde{\Delta}^2}{\sqrt{2}}(1 + n_r + n_l), \tag{B.4}$$

which always remain finite. Therefore, we observe the crucial property that this system shares with a non-relativistic Cooper pair, namely, the pair of relativistic fermions are bounded in pairs even for a weak attraction $\xi \ll 1$.

Another fundamental property that occurs in standard Cooper pairs is the presence of an energy gap between the paired energy level and the Fermi surface. This energy gap is responsible for the stability of Cooper pairs with respect to free fermion pairs and is proportional to the lattice Debye frequency $\Delta E \sim \hbar\omega_D$. In the relativistic regime, we observe that the energy gap is

$$\Delta E_{-n_r n_l} = 2\hbar\omega\,(n_r - n_l), \tag{B.5}$$

and therefore the only stable pair (i.e. $\Delta E \leqslant 0$) is that described by the spin-singlet state when $n_l \geqslant n_r$. In this sense we obtain a spin-singlet bound pair which clearly resembles the situation in standard Cooper pairs where the fermions are also in the singlet state. Furthermore, we can observe from this discussion that the relativistic gap is proportional to the Dirac string frequency $\Delta E \sim \hbar\omega$, which plays the role of the usual Debye frequency in superconducting materials. Finally, to take this comparison further, we should study the properties of the stable pair eigenstates in equation (B.3) and compare them to the non-relativistic Cooper pair features.

Spin degrees of freedom. In BCS theory, Cooper pairs display a singlet state in the spin degree of freedom. We observe in equation (B.3) that the stable bound fermionic pair state has also a spin-singlet component.

Orbital degrees of freedom. In BCS theory, Cooper pairs display a spherically symmetrical wavefunction with an onion-like layered structure. We directly observe from figure B2 that relativistic bound pair probability distribution $\rho^{\text{eff}}_{-n_r n_l}(r)$ displays a similar spherically symmetric onion-like structure.

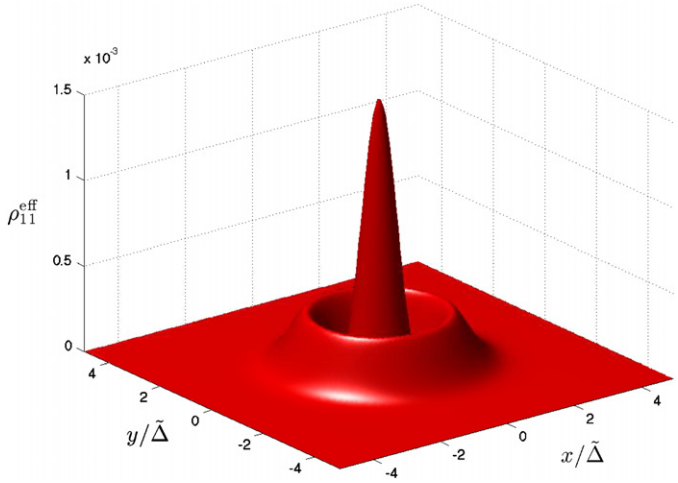

Figure B2. Spatial probability density profiles for weak coupling stable pairs $\rho^{\text{eff}}_{n_r n_l}(r) := \text{Tr}_{\text{spin}}(\langle \mathbf{r}|E^{\text{eff}}_{-n_r n_l}\rangle\langle E^{\text{eff}}_{-n_r n_l}|\mathbf{r}\rangle)$ with $n_l \geqslant n_r$. This figure corresponds to probability density $\rho^{\text{eff}}_{11}(r)$, with $r = |\mathbf{r}_1 - \mathbf{r}_2|/\sqrt{2}$.

B.2. Strong coupling regime

In this section we study the pairing properties of the two-body relativistic system in the strong coupling regime $\xi \lesssim 1$. In this limit we must consider the complete four-level structure of the system (see figure 1). In figure 3, we observe that two levels E_{2,n_r,n_l}, E_{3,n_r,n_l} become stable pairs with a certain gap $\Delta E_{2,n_r,n_l} < \Delta E_{3,n_r,n_l} < 0$. Therefore, the strong coupling gives rise to a couple of stable bound fermionic states, namely,

$$|E_{2,n_r,n_l}\rangle := \frac{1}{\Omega_{2n_r n_l}}(\mathrm{i}\beta_{2n_r n_l}|\uparrow\uparrow, n_r, n_l+1\rangle + \alpha_{2n_r n_l}|-\rangle|n_r, n_l\rangle + \mathrm{i}\delta_{2n_r n_l}|\downarrow\downarrow, n_r+1, n_l\rangle);$$
$$|E_{3,n_r,n_l}\rangle := \frac{1}{\Omega_{3n_r n_l}}(+\mathrm{i}\beta_{3n_r n_l}|\uparrow\uparrow, n_r, n_l+1\rangle + \alpha_{3n_r n_l}|-\rangle|n_r, n_l\rangle + \mathrm{i}\delta_{3n_r n_l}|\downarrow\downarrow, n_r+1, n_l\rangle), \tag{B.6}$$

whose spatial probability distribution $\rho_{jn_r n_l}(r)$ has been represented in figure B3 in the case of $n_r = n_l = 1$. We can clearly observe that the density profile preserves the spherically symmetric onion-like structure. Nonetheless, noteworthy differences arise with respect to the weak coupling regime (compare to the top figure B2).

Furthermore, these two stable states form a fermionic bound pair since the inter-particle distance is finite

$$\langle\Gamma\rangle_2 = \frac{\tilde{\Delta}^2}{\sqrt{2}}\left[(2+n_r+n_l) - \frac{\alpha^2_{2n_r n_l}}{\Omega^2_{2n_r n_l}}\right], \qquad \langle\Gamma\rangle_3 = \frac{\tilde{\Delta}^2}{\sqrt{2}}\left[(2+n_r+n_l) - \frac{\alpha^2_{3n_r n_l}}{\Omega^2_{3n_r n_l}}\right]. \tag{B.7}$$

We may conclude that the relativistic pairing mechanism leads to bound pairs in the strong coupling regime, which display substantial differences with respect to the weakly coupled bound states in equation (B.3). It follows from equations (B.6) that the bound pairs are not in a singlet state but rather in a linear superposition of different spin singlet and triplet states entangled with different orbital Fock states.

It is also instructive to compare the orbital degrees of freedom of bound pairs in the weak and strong coupling limits. The weakly coupled states in equation (B.3) are in orbital Fock states, which represent a certain number of vibrational phonons which are frozen in

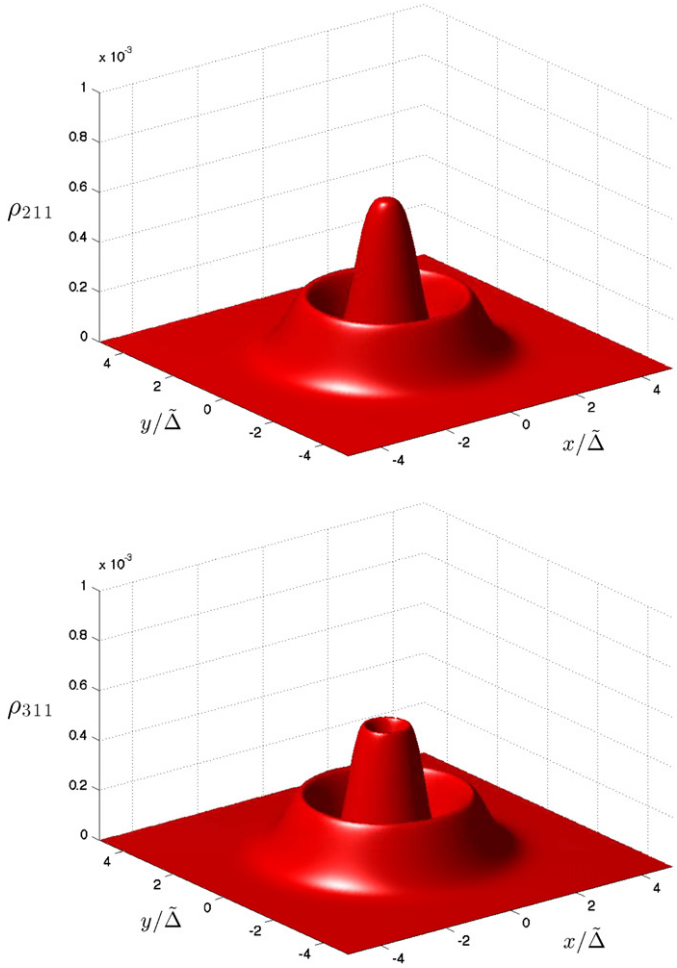

Figure B3. Spatial probability density profiles for strong coupling $\xi \lesssim 1$ stable pairs $\rho_{jn_rn_l}(r) := \mathrm{Tr}_{\mathrm{spin}}(\langle \mathbf{r}|E_{jn_rn_l}\rangle\langle E_{jn_rn_l}|\mathbf{r}\rangle)$ with $n_r = 1, n_l = 1$. Top figure corresponds to the probability density of the stable pair $\rho_{211}(r)$, with $r = |\mathbf{r}_1 - \mathbf{r}_2|/\sqrt{2}$. Bottom figure represents the probability density of the stable pair $\rho_{311}(r)$.

this limit. On the other hand, strongly coupled states in equations (B.6) cannot be described by a single Fock state, and therefore the vibrational phonons acquire a dynamical behavior $|n_r{+}1, n_l\rangle \leftrightarrows |n_r, n_l\rangle \leftrightarrows |n_r, n_l{+}1\rangle$, which is a clear sign of strong coupling in superconductors [55, 57]. We may conclude that the relativistic chiral phonons, responsible for the gluing mechanism, become unfrozen as the coupling becomes stronger and contribute to the effective attraction in a dynamic phenomenon. This is reminiscent of a (s, p)-wave symmetry of a SC order parameter. Similar types of superconducting states appear in some quantum liquids like superfluid He^3: the so-called A- and B-phases exhibit different patterns of spin-orbit symmetry breaking [58, 59]. Layered materials like the ruthenates also exhibit unusual symmetry properties like triplet superconductivity [60–62]. We also observe that the strong pairing mechanism leads to a couple of possible stable bound pairs (B.6), whereas the weak coupling only produces one stable bound pair. Furthermore, the energy gap displayed by the bound pairs also depends on the strength of the coupling.

References

[1] Einstein A, Podolsky B and Rosen N 1935 *Phys. Rev.* **47** 777
[2] Nielsen M and Chuang I 2000 *Quantum Computation and Quantum Information* (Cambridge: Cambridge University Press)
[3] Galindo A and Martin-Delgado M A 2002 *Rev. Mod. Phys.* **74** 347
[4] Horodecki R, Horodecki P, Horodecki M and Horodecki K 2007 *Rev. Mod. Phys.* at press arXiv: quant-ph/0702225
[5] Peres A and Terno D R 2004 *Rev. Mod. Phys.* **76** 93
[6] Plenio M B and Virmani S 2007 *Quantum Inf. Comput.* **7** 1
[7] Eisert J and Plenio M B 2003 *Int. J. Quantum Inf.* **1** 479
[8] Peres A, Scudo P F and Terno D R 2002 *Phys. Rev. Lett.* **88** 230402
[9] Czachor M 1997 *Phys. Rev* A **55** 72
[10] Gringrich R M and Adami C 2002 *Phys. Rev. Lett.* **89** 270402
[11] Alsing P M and Milburn G J 2002 *Quantum Inf. Comput.* **2** 487
[12] Ahn D, Lee H J, Moon Y H and Hwang S 2003 *Phys. Rev.* A **67** 012103
[13] Jordan T F, Shaji A and Sudarshan E C G 2005 *Phys. Rev.* A **73** 032104
[14] Lamata L, Martin-Delgado M A and Solano E 2006 *Phys. Rev. Lett.* **97** 250502
[15] Pachos J and Solano E 2003 *Quantum Inf. Comput.* **3** 115
[16] Lamata L, Leon J and Solano E 2006 *Phys. Rev.* A **73** 012335
[17] Greiner W 2000 *Relativistic Quantum Mechanics. Wave Equations* (Berlin: Springer)
[18] Barut A O and Komy S 1985 *Fortsch. Phys.* **33** 6
[19] Ito D, Mori K and Carrieri E 1967 *Nuovo Cimento* A **51** 1119
[20] Moshinsky M and Szcepaniak A 1989 *J. Phys. A: Math. Gen.* **22** L817
[21] Moshinsky M, Loyola G and Villegas C 1990 *J. Math. Phys.* **32** 373
[22] Kwiat P G 1997 *J. Mod. Opt.* **44** 2173
[23] Scully M O and Zubairy M S 2002 *Quantum Optics* (Cambridge: Oxford University Press)
[24] Perelomov A M 1972 *Commun. Math. Phys.* **26** 222
[25] Cooper L N 1956 *Phys. Rev.* **104** 1189
[26] Moshinsky M and Loyola G 1993 *Found. Phys.* **23** 197
[27] González A, Loyola G and Moshinsky M 1994 *Rev. Mex. Fis.* **40** 12
[28] Bermudez A, Martin-Delgado M A and Solano E 2007 *Phys. Rev.* A **76** 041801
[29] Bermudez A, Martin-Delgado M A and Luis A 2008 *Phys. Rev.* A **77** 033832
[30] Bermudez A, Martin-Delgado M A and Solano E 2007 *Phys. Rev. Lett* **99** 123602
[31] Bermudez A, Martin-Delgado M A and Luis A 2008 *Phys. Rev.* A **77** 063815
[32] Jaynes E T and Cummings F W 1963 *Proc. IEEE* **51** 89
[33] Haroche S and Raimond J M 2006 *Exploring the Quantum* (New York: Oxford University Press)
[34] Leibfried D, Blatt R, Monroe C and Wineland D 2003 *Rev. Mod. Phys.* **75** 281
[35] Tavis M and Cummings F W 1968 *Phys. Rev.* **170** 379
[36] Swain S 1972 *J. Phys. A: Gen. Phys.* **5** L3
[37] Bell J S 1964 *Physics* **1** 195
[38] Radmore P and Knight P L 1982 *J. Phys. B: At. Mol. Phys.* **15** 561
[39] Harris S E, Field J E and Imamoglou A 1990 *Phys. Rev. Lett.* **64** 1107
[40] Glauber R J 1963 *Phys. Rev.* **130** 2529
Glauber R J 1963 *Phys. Rev.* **131** 2766
[41] Gerry C C 1993 *J. Mod. Opt.* **40** 1053
[42] Kwiat P G and Weinfurter H 1998 *Phys. Rev.* A **58** 2623
[43] Barreiro J T, Langford N, Peters N A and Kwiat P G 2005 *Phys. Rev. Lett.* **95** 260501
[44] Davidovitch L 1996 *Rev. Mod. Phys.* **68** 127
[45] Kok P, Ralph T C and Milburn G 2005 *Quantum Inf. Comput.* **5** 239
[46] Zanardi P and Rasseti M 1997 *Phys. Rev. Lett.* **79** 3306
[47] Lidar D A, Chuang I L and Whaley K B 1998 *Phys. Rev. Lett.* **81** 2549
[48] Perelomov A 1986 *Generalized Coherent States and Their Applications* (Berlin: Springer)
[49] Puri R R 2001 *Mathematical Methods of Quantum Optics* (Berlin: Springer)
[50] Wodkiewicz K and Eberly J H 1985 *J. Opt. Soc. Am.* B **2** 458
[51] Buzek V and Quang T 1989 *J. Opt. Soc. Am.* B **6** 2447
[52] Campos R A, Saleh B E A and Teich M C 1989 *Phys. Rev.* A **40** 1371
[53] Frölich H 1950 *Phys. Rev.* **79** 845

[54] Bardeen J, Cooper L N and Schrieffer J R 1957 *Phys. Rev.* **108** 1175
[55] Migdal A B 1958 *Zh. Eksp. Teor. Fiz.* **34** 1438
Migdal A B 1958 *Sov. Phys. JETP* **7** 996
[56] Eliashberg G M 1960 *Zh. Eksp. Teor. Fiz.* **38** 966
Eliashberg G M 1960 *Sov. Phys. JETP* **11** 696 (Engl. Transl.)
Eliashberg G M 1960 *Zh. Eksp. Teor. Fiz.* **39** 1437
Eliashberg G M 1960 *Sov. Phys. JETP* **12** 1000 (Engl. Transl.)
[57] Carbotte J P 1990 *Rev. Mod. Phys.* **62** 1027
[58] Osheroff D D, Richardson R C and Lee D M 1972 *Phys. Rev. Lett.* **28** 885
[59] Leggett A J 1975 *Rev. Mod. Phys.* **47** 331
[60] Maeno Y *et al* 1994 *Nature* **372** 532
[61] Rice T M and Sigrist M 1995 *J. Phys. Condens. Matter* **7** L643
[62] Baskaran G 1996 *Physica* B **223–224** 490